Structural Characteristics of Antimony Sulfide Layers

V. N. VERTSNER, B. V. GORBUNOV AND IA. A. OKSMAN

State Optics Institute

(Submitted to JETP editor November 27, 1956)

J. Exptl. Theoret. Phys. (U.S.S.R.) 32, 957-961 (May, 1957)

The nature of the sensitization processes in Sb_2S_3 layers was investigated by means of electron diffraction. It was established that when a layer condenses on a heated backing it consists of an amorphous mass of antimony sulfide and a thin surface film of Sb_2O_3. The dependence of the orientation of the small oxide crystals on the condensation temperature was determined. It is suggested that the photosensitivity of the investigated layers is determined by the crystalline oxide which provides additional trapping centers for the current carriers.

THE PHOTOELECTRIC PROPERTIES of antimony sulfide layers produced by vacuum evaporation are determined principally by the condensation conditions. In distinction from the majority of sulfides and selenides, the properties of the layer are well reproducible; this suggests that the sensitization processes in this instance are less complex than in PbS, for example.

Since photosensitivity is principally dependent on temperature two thermal activation mechanisms can be conceived. The first process is associated with crystallization of the basic material; the second is associated with the formation of oxides. The experiments which will be described here were intended, first, to determine the character of the activation processes and, secondly, to indicate the relation between the structural characteristics of the layers and their photoelectric properties. The second purpose required a study of the photoelectric properties of the layers. The principal results of our investigation will be presented here.

The resistivity of the layers lies between 10^{10} and 10^{13} ohm-cm and shows little dependence on the temperature of the backing or the subsequent heat treatment. The material of the contacts has almost no effect on the resistance of the specimens. The sign of the thermal emf indicates the predominance of p-type conductivity. Photoconduction is observed only in layers evaporated on a backing which had been heated to 100–120° C, or on a backing at room temperature but subsequently heating for 1 to 2 minutes to 250–300° C in air. The latter method of activation yields less stable and less reproducible results.

The curves in Fig. 1 give an idea of the spectral characteristics of the photosensitivity at room temperature. These curves were not converted to
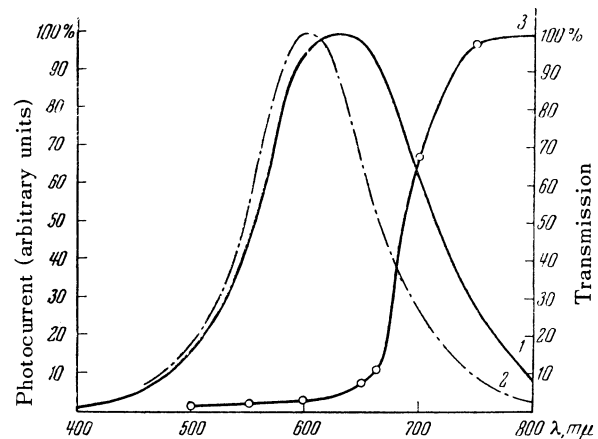

FIG. 1. Spectral distribution of photosensitivity in a layer of Sb_2S_3 at room temperature. 1—field along the specimen; 2—field at right angles to specimen; 3—optical transmission of specimen.

units of incident energy (an incandescent lamp being used as the source). The most important property of the curves is that in the strong absorption region they are independent of the direction of the electric field. If it is assumed that the carrier drift distance is considerably smaller than the layer thickness, then when the photoconductivity is measured perpendicular to the surface layer, under strongly absorbed radiation, the resistance will vary only on the surface of the specimen. Measurements along the layer should not be influenced by the same circumstance and in this case the photoconductivity curve in the strong absorption region should reveal a smaller decline.

Since the short-wave ends of the curves are of identical character we can assume that carrier drift in this case exceeds the layer thickness (1–2μ).

A temperature rise from 20 to 100° C results in an exponential rise of both the dark current and

the photocurrent. The corresponding activation energies are approximately 0.3 and 0.1 ev and vary with the specimens.

The photoconductivity relaxation time measured transversely is usually somewhat greater than when measured along the layer; its absolute value under low illumination amounts to a fraction of a second. Relaxation is characterized by both a fast and a slow process; as with all high-resistance semiconductors the latter process is apparently associated with the thermal liberation of carriers from deep traps.

The introduction of donors (Cu, Sb, Cd) does not essentially alter the properties of the layers. A small quantity of antimony oxide in the evaporated material increases the dark resistance.

It should be noted that antimony sulfide layers are of considerable practical interest because they are used extensively in "vidicon" photoconductive television camera tubes [1,2].

We have investigated two kinds of antimony sulfide layers: thin free films and ordinary layers on glass. The thin films were prepared by vacuum evaporation of Sb_2S_3 which condensed on organic backings at room temperature, $100°$ C and in some instances a little above or below $100°$ C. Backings at room temperature are designated as "cold".

All electron diffraction patterns from such layers are characterized by a common strong background. As the temperature of the backing was raised there was an increase in the definition, intensity, and number of observed reflections. Fig. 2 is the electron diffraction pattern of a layer of Sb_2S_3 evaporated on a hot backing ($100°$ C). Table 1 gives the interplanar spacings that were calculated according to diffraction patterns from thin Sb_2S_3 layers evaporated on cold and $100°$ C backings. The interplanar spacings of Sb_2O_3 found in structural tables are also given. A comparison shows that in both cases the reflections were produced by small Sb_2O_3 crystals.

Thus thin films produced by vacuum evaporation of Sb_2S_3 contain amorphous Sb_2S_3 and crystalline Sb_2O_3. The presence of amorphous Sb_2S_3 in the
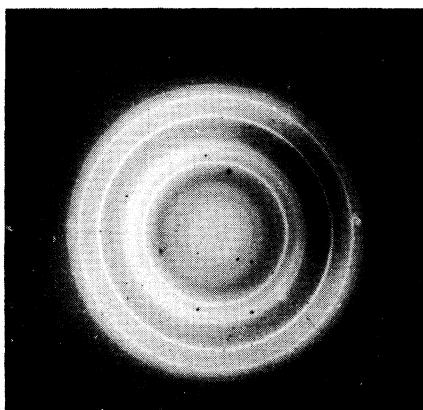

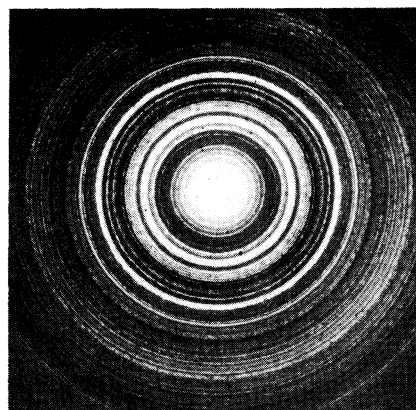FIG. 2. Electron diffraction pattern of a Sb_2S_3 film evaporated on a cold backing.

FIG. 3. Electron diffraction pattern of a Sb_2S_3 film heated at $300°$ C for 2 minutes.
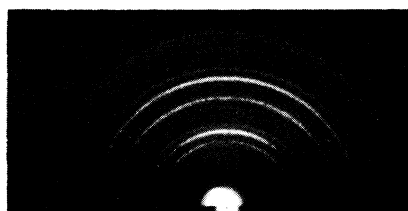

FIG. 4. Electron diffraction pattern of a Sb_2S_3 layer evaporated on cold glass and heated at $300°$ C for 2 minutes.
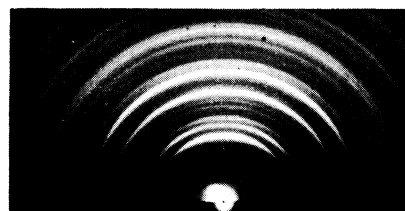

FIG. 5. Electron diffraction pattern of a Sb_2S_3 layer evaporated on hot glass and heated at $300°$ C for 2 minutes.

TABLE I. Interplanar spacings calculated from electron diffraction patterns
of thin Sb_2S_3 layers evaporated on cold backings and backings heated to $100°$ C.

Sb₂S₃ layer on cold backing		Sb₂S₃ layer on hot backing		Tabulated values (Sb₂O₃)	
d, A	Intensity	d, A	Intensity	d, A	Intensity in %
		6.4	strong	6.4	10
3.26	strong	3.22	v. strong	3.22	100
2.78	weak	2.82	medium	2.78	30
		2.58	medium	2.56	8
		2.31	v. weak		
		2.16	v. weak		
1.96	weak	1.98	strong	1.96	50
1.68	weak	1.70	strong	1.68	50
		1.64	weak	1.61	10
		1.58	medium	1.56	10
				1.45	2
		1.39	v. weak	1.39	6
				1.36	4
		1.29	v. weak	1.28	15
		1.26	v. weak	1.25	10

TABLE II. Interplanar spacing calculated from electron diffraction patterns
of Sb_2S_3 films heated at $300°$ C for two minutes.

Calculated values		Tabulated values					
		Sb₂O₃		Sb₂S₃		Sb	
d, A	Intensity	d, A	Intensity in %	d, A	Intensity in %	d, A	Intensity in %
				8.2	6		
7.95	medium						
6.35	strong	6.4	10				
5.61	medium			5.6	23		
5.02	medium			5.0	46		
3.93	medium			3.97	2.3		
3.64	medium					3.71	15
3.55	medium			3.57	100		
3.46	medium						
3.22	v. strong	3.22	100				
3.12	medium					3.10	100
3.04	v. strong			3.02	86		
2.82	weak						
2.76	strong	2.78	30	2.75	86		
2.67	medium			2.66	34		
2.60	medium			2.60	6		
2.52	medium	2.56	8	2.50	34		
2.42	medium			2.42	23		
2.28	weak					2.24	63
2.22				2.23	29	2.14	63
2.18	weak						
2.10	strong			2.09	40		

original films is confirmed by electron diffraction patterns of antimony sulfide films heated at $300°$ C for 2 minutes (the original films were produced by condensation on $100°$ backings). Fig. 3 and Table 2 show that the amorphous antimony sulfide of the original layer is well crystallized under these con-

ditions. In addition to the Sb_2S_3 the layers contain Sb_2O_3, possibly some metallic antimony and still unidentified compounds, whose interplanar spacings are also given in Table 2.

Thick antimony sulfide layers on glass are crystallized somewhat differently than the condensate on organic films. The reflection patterns show a

TABLE III. Interplanar spacings calculated from electron diffraction patterns of Sb_2S_3 layers on glass heated for 2 minutes at 300° C.

Calculated values		Tabulated values for Sb_2O_3	
d, Å	Intensity	d, Å	Intensity in %
4.08	extr. weak		
3.20	v. strong	3.22	100
2.84	strong	2.78	30
2.57	medium	2.56	8
2.3	weak		
2.16	weak		
1.96	v. strong	1.96	50
1.91*	extr. weak		
1.70	v. strong	1.68	50
1.62	extr. weak	1.61	10
1.57	medium	1.56	10
1.46	weak	1.45	2
1.39	extr. weak	1.394	6
1.37	medium	1.36	4
1.32	extr. weak		
1.28	medium	1.28	15
1.25	weak-med.	1.25	10
1.18	extr. weak	1.18	1
1.14	medium	1.138	4
1.08	strong	1.073	8

*For Sb_2S_3 the $d = 1.92$ reflection has 100% intensity.

very strong background which is evidently caused by scattering from amorphous Sb_2S_3. The reflections are very broad. The broadening and the background are much less apparent for layers evaporated on hot backings. When both types of layers are heated for 2 minutes at 300° C the diffraction patterns show reflection arcs, which are evidence of the formation of oriented crystals on the surface of the sublimate. Table 3 and Figs. 4 and 5 show that the Sb_2O_3 crystals have different orientations in these layers.

In the case of samples produced by heating sensitive layers previously evaporated on a hot backing the crystals of cubic Sb_2O_3 are oriented predominantly with the (111) atomic planes parallel to the backing. Heating of insensitive layers orients the oxide crystals with cube faces (100 planes) parallel to the backing. The orientation of Sb_2O_3 crys-

tals which we observed in heated sensitive layers of Sb_2S_3 coincides with the orientation of BiO crystals in oxidized thin layers of similar compounds— Bi_2Se_3 and Bi_2Te_3[3].

We also obtained Debye X-ray patterns of the original material and of the material of layers in the form of powders scraped from glass and containing the original and oxidized Sb_2S_3 sublimates. The X-ray patterns of the original sublimates revealed only individual and very diffuse reflections. This is confirmation that the material of such layers is amorphous. After heating, the powder taken from the glass produced X-ray patterns with clear strong reflections. The system of reflections was identical with that obtained in X-ray patterns of the original material and corresponded to Sb_2S_3.

The absence of Sb_2O_3 lines in the X-ray patterns and the absence of reflections from Sb_2O_3 in the electron reflection patterns is confirmation that the oxide phase is a small fraction of the layer material and is mainly concentrated on its surface.

CONCLUSIONS

Structural studies show that thin layers of photosensitive antimony sulfide consist mainly of amorphous Sb_2S_3, an oxide surface film composed of cubic Sb_2O_3 crystals, and possibly metallic antimony. Heating of the sublimates is accompanied by growth of the crystals. Crystals of the oxide phase which form on the surface have very different orientations depending on the temperature of the backing during the condensation process. It can thus be assumed that photosensitivity is associated not with crystallization of the bulk of the layer but rather with the processes that accompany the formation of the oxide. The literature contains detailed studies of the sensitization of layers by impurities which increase carrier lifetime[4]. It is also known that in many sulfides and selenides oxygen acts as such an impurity. It is thus reasonable to interpret our findings as follows:

The formation of a thin film of definitely oriented oxide crystals on the surface results in the appearance of new recombination centers in antimony sulfide layers. The influence of the oxide surface film on the volume photoconductivity of the photolayers can be attributed to the thinness of the layers and to the large carrier drift length.

Any free antimony contained in the layers is unlikely to act as a sensitizer, as experiments with

the introduction of donor impurities have produced negative results.

In conclusion the authors must thank Academician A. A. Lebedev for his interest and valuable suggestions. The authors are also grateful to G. V. Anan'eva and A. I. Kuznetsov for their assistance.

[1] Artem'ev, Sokolov and Temiriazeva, Radiotekhn. i Elektronika (Radio Engg. and Electronics) 1, 245 (1956).

[2] Forgue, Goodrich and Cope, RCA Rev. 12, 335 (1951).

[3] S. A. Semiletov and Z. G. Pinsker, J. Tech. Phys. (U.S.S.R.) 25, 2336 (1955).

[4] A. Rose, Phys. Rev. 97, (1955).

Translated by I. Emin
210

Energy Distribution of Neutrons Emitted from Beryllium Bombarded by 680 Mev Protons

V. KISELEV AND V. B. FLIAGIN

Joint Institute for Nuclear Research

(Submitted to JETP editor November 29, 1956)

J. Exptl. Theoret. Phys. (U.S.S.R.) 32, 962-964 (May, 1957)

The neutron energy spectra were measured at angles of 0 and 18° in the laboratory system. A peak not observed at lower primary-proton energies was detected in the 100—400 Mev region. The existence of this peak is explained by π-meson production processes.

THE PRESENT NOTE is to describe one of the experiments carried out to investigate the main characteristics of the fast neutron beams formed when beryllium targets are bombarded by 680-Mev protons.

In the present experiment the target was placed inside the synchro-cyclotron chamber and was 2.5 cm thick. The experiment was performed at angles $\theta = 0°$ and $\theta = 18°$ between the neutron beam and the direction of the velocity of the protons impinging on the target. The neutron energy distribution was investigated by determining the energy spectra of the recoil protons, emitted at a 30° laboratory angle, as a result of elastic $n-p$ scattering. For this purpose, paraffin or graphite scatterers were placed in the path of the neutron beam; the effect due to hydrogen was determined from the difference between the effects of these two scatterers.

The measurements were performed principally by the differential method. In this case the detector, a telescope with four scintillation counters (three were connected for coincidence, the fourth for anti-coincidence), was used to measure the intensity of the recoil proton current in some relatively narrow energy interval. The width of this interval and its position on the energy scale were fixed by means

of copper and tungsten filters, placed between the third and fourth and between the second and third counters, respectively. A system of controlling experiments made it possible to make all the necessary corrections, in particular to take into account the loss of protons in filters, their scattering in the scintillators, etc.

The main source of error in our experiment could have been the admixture of charged particles emitted from the following reactions in the scatterer:

$$n + p \rightarrow \pi^0 + (n + p); \quad n + p \rightarrow \pi^- + p + p;$$

$$n + p \rightarrow \pi^+ + n + n.$$
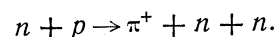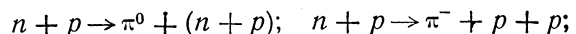
The corrections related to meson production processes included only in the high energy part of the neutron spectrum ($E_n > 450$ Mev), for which Kazarinov and Simonov, in a special experiment[1], have measured the integral $\pi^\pm$-meson yield from these reactions. Unfortunately, there are no experimental data on the energy spectrum of $\pi^\pm$-mesons formed in $n-p$ collisions. These corrections have therefore been calculated on the assumption that the energy distribution of the $\pi^\pm$-mesons corresponding to different incident neutron energies has a form similar to the spectra of $\pi^\pm$-mesons from the